

Exact treatment of Pauli exclusion effects in (p,p') reactions

E.J. Stephenson

Indiana University Cyclotron Facility, Bloomington, Indiana 47408

R.C. Johnson

Department of Physics, University of Surrey, Guildford, Surrey GU2 5XH, UK

F. Sammarruca

Department of Physics, University of Idaho, Moscow, Idaho 83844

Abstract: This paper presents the first calculations of proton inelastic scattering in which the medium effect of Pauli blocking is included through an exact, rather than angle averaged, operator. This improvement is important in the isoscalar channel at proton energies near 100 MeV and fades as the energy rises. However, processes that emphasize finite-range exchange (such as $0^+ \rightarrow 0^-$ reactions) still see significant effects at 200 MeV. The results depend on the directions of the incident and struck nucleon momenta that produce the most important contributions to the DWBA integral at each scattering angle.

I. Introduction

Proton elastic and inelastic scattering at energies above 100 MeV are usually described by distorted-wave calculations based on an effective nucleon-nucleon (NN) interaction. When the interaction with the projectile proton is summed, or “folded,” over all the nucleons in the target, the resulting potential can be used to describe elastic scattering. In addition, the same effective NN interaction becomes the transition potential that connects to excited states of the target when the struck nucleon moves to a new shell-model orbit, creating a particle-hole pair. The many-body effects of the nuclear medium are usually incorporated through modifications to this effective NN interaction that depend on the local nuclear density.

Systematic studies [1–5] have shown that one important part of the many-body effects is Pauli blocking, particularly at the lower energies in this range. In this case, a projectile nucleon travelling through the nuclear medium experiences a potential that arises from virtual NN scattering, but only to intermediate states for which both of the nucleons involved have momenta above the Fermi momentum [6]. This restriction is included through a projection operator in the Bethe-Goldstone equation for the G -matrix elements that describe the effective NN interaction inside the nuclear medium.

The usual practice is to average this Pauli projection operator over the intermediate state scattering angle. It has been argued that this spherical approximation is adequate for the central and spin-orbit terms in the effective interaction [7]. If this approximation

is removed, new G -matrix elements appear [7–10]. While remaining diagonal in total spin S and isospin T , the angular dependence allows coupled G -matrix elements that connect partial wave states where $J \neq J'$ and $\ell \neq \ell'$ beyond the $|\ell - \ell'| = 2$ coupling required by the tensor interaction.

In a recent calculation of the G -matrix [10], we observed that these new couplings in J and ℓ generate only small matrix elements, but the variation of M , the projection of the total angular momentum J , produces changes in the G -matrix elements that are similar in size to the Pauli blocking effect itself. Thus it seems appropriate to inquire whether it is possible to observe these differences between the exact and spherical Pauli operators in selected nuclear reactions, and in particular in their spin observables. Proton inelastic scattering offers a rich set of polarization observables, especially considering polarization transfer, that reflect the spin dependence of the effective NN interaction itself. Calculations that have considered only how the binding energy of nuclear matter is affected by the change from a spherical to an exact treatment of Pauli blocking show very small changes [8,9].

The dependence on M has been considered previously in calculations of deuteron binding in the presence of the nuclear medium [11]. While Pauli blocking reduces the deuteron binding energy, the amount depends on whether the projection of the deuteron's spin 1, $|M|$, is 0 or 1 when the quantization axis is taken along the direction of motion of the deuteron through nuclear matter. This difference generates a momentum-dependent T_P tensor potential in the deuteron-nucleus optical model. Optical model calculations have shown that T_P effects are best distinguished from those of a T_R tensor potential when the deuteron elastic scattering angular distribution is far-side dominated. In this case the orbiting trajectories make the deuteron's momentum nearly perpendicular to the radius from the center of the target when the deuteron is in the region of the nuclear surface [12]. Measurements of observables such as $X_2 = (2A_{xx} + A_{yy})/\sqrt{3}$ where spin-orbit effects are suppressed [13] are still insufficient to demonstrate unambiguously the existence of such a T_P potential, in part because it is necessary to also consider breakup channel coupling and the necessary computer programs to incorporate both do not exist.

In this paper, we begin with the G -matrix described in Ref. [10]. The important features of the calculation of the G -matrix elements are reviewed in Section II where we point out the aspects crucial for the reaction calculations. In order to use this effective interaction in distorted-wave calculations with presently-available computer programs, we must transform the matrix elements to a coordinate-space representation using a sum of Yukawa functions. In contrast to the single-step transformation described in Ref. [5], we will first convert the partial-wave matrix elements to angular distributions of the NN scattering amplitudes (see Section III). In the process, we will introduce an expansion of the new G -matrix elements in which the lowest order recovers the result for a spherical Pauli blocking operator. The coefficients of the Yukawa expansion will then be determined from a fit to these amplitudes. For the spherical Pauli operator, this produces the same result as the previous method [5]. In general, the new elements of the G -matrix require a larger range of spin operators than normally appears for NN scattering. Since these new operators are not available in existing distorted-wave programs, we did not include their contributions to proton-induced inelastic scattering.

In these calculations, it is natural to quantize along the direction of the momentum of the system. In nuclear matter, this is the momentum of the projectile, as noted earlier for the case of the deuteron. For this choice, large differences were seen previously for g -matrix elements with different values of M [10]. For the effective interaction that enters into elastic and inelastic scattering, it is also possible to choose as the system momentum the sum of the momenta of the incident and struck nucleons. For a reaction whose product is observed at a particular scattering angle, it is no longer required by symmetry that this sum average to the projectile direction. The question of what is the most important direction for this sum also arises when combining the direct and exchange parts of the effective NN interaction when making a zero-range DWIA calculation. In Appendix B of Ref. [5] we presented a scheme in which the struck nucleon's momentum is chosen so that, at any given momentum transfer (associated with a particular scattering angle), the scattering has on-shell kinematics. In the limit where the reaction Q -value vanishes and the recoil of the target is neglected, this scheme places the momentum of the two-nucleon system (sum of the incident and struck nucleon momenta) pointing in the reaction plane at an angle that is half of the scattering angle. Thus the best choice for nucleon-induced reactions may not be the same as for nucleons travelling through nuclear matter. As part of the development described here, we will explore both of these options as a test of the importance of this issue of kinematics for the treatment of Pauli blocking.

In Section III we will compare the exact and spherical treatments of the Pauli blocking operator for representative nuclear transitions at 100 and 200 MeV. We will include a comparison to the free, or density-independent, effective interaction to help gauge the importance of the exact treatment relative to the effect of not including Pauli blocking at all. We will show that this relative importance rises at lower bombarding energies.

We will also compare with measurements of the cross section and analyzing power to illustrate these new effects in relation to the quality of the reproduction of these data. Pauli blocking has its largest effects on the isoscalar central and spin-orbit terms in the effective interaction. These terms are well tested by a comparison to elastic proton scattering or transitions to natural-parity excited states. Since the two alternatives for the choice of the system momentum arise out of a consideration of exchange between the projectile and the struck nucleon, we will include calculations for a $0^+ \rightarrow 0^-$ transition. In this spin structure there is no analyzing power (in a plane-wave calculation) unless there is finite-range exchange in the distorted-wave calculation. So here we might expect to be sensitive to this issue.

Pauli blocking is only one process that is important in the calculation of the effective interaction in the nuclear medium. Others, such as the effects of strong relativistic mean fields [10,14,15] and coupling to Δ -resonances [16], increase the repulsion in the nuclear medium just as does Pauli blocking [17]. In a complete treatment, these should be properly considered, along with the attraction expected to arise from many-body forces. Thus we will not expect that a set of calculations that includes only Pauli effects will produce good agreement with the data. However, any critical evaluation of any of these medium effects requires that the treatment of Pauli blocking not introduce systematic errors large enough to affect our interpretation when agreement with data is considered. We will show that in this energy range one must include an exact treatment of the angular dependence of the

blocking operator in order to meet this standard.

II. Calculation of the G -matrix elements

The Brueckner-Bethe-Goldstone equation [18–21] describes scattering of two nucleons in nuclear matter. The presence of the (infinite) medium is accounted for through Pauli blocking and a mean field arising from the interactions with all the other nucleons. It is convenient to express the momenta of the two nucleons, \mathbf{k}_1 and \mathbf{k}_2 , in terms of the relative and center-of-mass motion as

$$\mathbf{k} = (\mathbf{k}_1 - \mathbf{k}_2)/2 \quad (1a)$$

$$\mathbf{P} = (\mathbf{k}_1 + \mathbf{k}_2)/2 . \quad (1b)$$

The total or center-of-mass momentum \mathbf{P} is conserved in the scattering process.

In strict analogy with free-space scattering, the Bethe-Goldstone equation is given by

$$G(\vec{q}', \vec{q}, \vec{P}, E_0) = V(\vec{q}', \vec{q}) \quad (2)$$

$$+ \int \frac{d^3K}{(2\pi)^3} V(\vec{q}', \vec{K}) \frac{Q(\vec{K}, \vec{P})}{E_0 - E(\vec{P}, \vec{K})} G(\vec{K}, \vec{q}, \vec{P}, E_0) ,$$

where V is the two-body potential. The energy of the two-particle system, E (with E_0 its initial value), includes kinetic energy and the potential energy generated by the mean field. The latter is determined in a separate self-consistent calculation of nuclear matter properties and conveniently parametrized in terms of effective masses [5].

The Pauli projection operator Q selects intermediate states only when both momenta lie above the Fermi momentum k_F :

$$Q(\mathbf{k}, \mathbf{P}, k_F) = \begin{cases} 1 & \text{if } k_1, k_2 > k_F \\ 0 & \text{otherwise} \end{cases} \quad (3)$$

Visualizing the (sharp) Fermi surface as a sphere of radius k_F , the condition above imposes the requirement that the tips of the \mathbf{k}_1 and \mathbf{k}_2 vectors lie outside the sphere. For applications to real nuclei, k_F is treated as a function of the local nuclear density

$$\rho(r) = \frac{2k_F^3(r)}{3\pi^2} . \quad (4)$$

The matrix elements for the exact Pauli operator may be written in a partial wave basis as

$$\langle (\ell' S) J' M | Q(k, P, k_F) | (\ell S) J M \rangle \quad (5)$$

$$= \sum_{m_\ell, m_S} \langle \ell' m_\ell S m_S | J' M \rangle \langle J M | \ell m_\ell S m_S \rangle \langle \ell' m_\ell | Q(k, P, k_F) | \ell m_\ell \rangle ,$$

where

$$\langle \ell' m_\ell | Q(k, P, k_F) | \ell m_\ell \rangle = \int d\Omega Y_{\ell' m_\ell}^*(\Omega) Y_{\ell m_\ell}(\Omega) \Theta(|\mathbf{k}_1| - k_F) \Theta(|\mathbf{k}_2| - k_F) . \quad (6)$$

The step functions destroy the orthogonality that would otherwise exist for the spherical harmonics in the integral. This allows couplings to appear where $\ell \neq \ell'$ and, through the recoupling coefficients in the summation, to couplings where $J \neq J'$. Since the step functions involve the polar angle θ and not the azimuthal angle ϕ , mixing does not arise between different values of m_ℓ and $m_{\ell'}$, and this carries over into the values of M and M' . This restriction is already incorporated into Eqs. (5) and (6). Thus we finally must consider a G -matrix element whose general spin and isospin structure is

$$G = \langle \ell' J' | G_M^{ST} | \ell J \rangle . \quad (7)$$

The G -matrix elements that we will use here were generated from a free-space NN interaction that is a modified version of the Bonn-B potential [17]. Pseudo-vector coupling is used for the pion, and the σ -meson coupling is allowed to assume different values as a function of isospin and vary over a limited range in the lowest partial waves. The masses, coupling constants, and cutoff parameters may be found in Ref. [5]. All of these parameters of the force were adjusted to match the phase shift analysis results from the Nijmegen group at all energies up to 325 MeV [22].

The number of coupled channels in Eq. (7) increases with M as it becomes possible to incorporate larger values of J . However, the M -dependence decreases with increasing J [10] and we were able to ignore medium effects on partial waves where $J, J' > 6$ because of the small size of these effects.

III. Transformation of the G -matrix to coordinate space

We will begin this section with a description of the general formulas that connect the expanded G -matrix of Eq. (7) to NN scattering amplitudes, regardless of the complexity of the coupling. Next, we will summarize the simplified forms used for the calculations reported here, explaining in each case what features have been left out.

The G -matrix elements of Eq. (7), $\langle \ell' J' M | G^{ST}(\vec{P}) | \ell J M \rangle$, may be expanded as a function of L where L is the angular momentum that recouples J to J' using the coefficients $G^{LST}(\ell' J', \ell J, P)$. While the z -axis in Eq. (6) was taken to lie along the projectile momentum and thus \vec{P} did not appear in Eq. (7), here we include \vec{P} explicitly to generalize this result for reactions. Thus,

$$\langle \ell' J' M | G^{ST}(\vec{P}) | \ell J M \rangle = \sqrt{4\pi} \sum_{L\Lambda} \langle J' M, L\Lambda | J M \rangle \hat{L} Y_{L\Lambda}(\vec{P}) G^{LST}(\ell' J', \ell J, P) . \quad (8)$$

Equation (8) can be inverted to yield the expansion coefficients

$$G^{LST}(\ell' J', \ell J, P) = \frac{1}{\hat{j}^2} \sum_M \langle J' M, L0 | J M \rangle \langle \ell' J' M | G^{ST}(\vec{P}) | \ell J M \rangle . \quad (9)$$

Since \vec{P} is the average momentum of the colliding nucleons, it is invariant under their interchange. So the anti-symmetrized G -matrix element is obtained by subtracting from

Eq. (9) the same terms that are there but with an additional phase of $(-)^{\ell+S+T} = -1$, leaving the set that normally describes NN scattering. L takes on only even values.

We would now like to convert the representation from partial wave angular momenta to amplitudes as a function of angle. In the process, we wish to separate the parts of G associated with the central, spin-orbit, and tensor operators usually used to describe the spin structure of the NN scattering amplitudes. In particular, we want to consider the form

$$G^{LST} = G_C^{LST} + \delta_{S1} [G_{LS}^{L1T} (\vec{\sigma}_1 + \vec{\sigma}_2) \cdot \hat{n} + G_{TD}^{L1T} S_{12}(\hat{q}) + G_{TX}^{L1T} S_{12}(\hat{Q})] \quad (10)$$

where $\vec{q} = \vec{k}'_1 - \vec{k}_1$ is the momentum transfer, \hat{n} is the normal to the scattering plane, and $\hat{Q} = \hat{q} \times \hat{n}$. Each of the G_i^{LST} is a function of angle. The subscript indicates the part of the NN amplitude, using C for central, both $S = 0$ and $S = 1$, LS for spin-orbit, and TD and TX for the ‘‘direct’’ and ‘‘exchange’’ parts of the tensor interaction.

The coefficients of Eq. (10) are simply related to an expansion in spherical harmonics where the coefficients $G_{kq}^{ST}(\vec{k}, \vec{k}', L)$ can be obtained from the coefficients of of Eq. (9) for all spin operators through

$$G_{kq}^{ST}(\vec{k}, \vec{k}', L) = \text{Trace} (G^{LST} \tau_{kq}) \quad (11)$$

where

$$\langle S\sigma' | \tau_{kq} | S\sigma \rangle = \hat{k} \langle S\sigma, kq | S\sigma' \rangle \quad (12)$$

and k runs from 0 to $2S$. For the coefficients shown in Eq. (10),

$$G_C^{LST} = \hat{S}^{-2} G_{00}^{ST}(\vec{k}, \vec{k}', L) \quad (13)$$

$$G_{LS}^{L1T} = \frac{\sqrt{2\pi}}{6} \sum_q Y_{1q}^*(\vec{n}) G_{1q}^{1T}(\vec{k}, \vec{k}', L) \quad (14)$$

$$G_{TD}^{L1T} - \frac{1}{2} G_{TX}^{L1T} = \frac{\sqrt{10\pi}}{30} \sum_q Y_{2q}^*(\vec{q}) G_{2q}^{1T}(\vec{k}, \vec{k}', L) \quad (15)$$

$$-\frac{1}{2} G_{TD}^{L1T} + G_{TX}^{L1T} = \frac{\sqrt{10\pi}}{30} \sum_q Y_{2q}^*(\vec{Q}) G_{2q}^{1T}(\vec{k}, \vec{k}', L) . \quad (16)$$

The $G_{kq}^{ST}(\vec{k}, \vec{k}', L)$ are functions of the scattering angle through the directions of \vec{k} and \vec{k}' . They are obtained from

$$\begin{aligned} G_{kq}^{ST}(\vec{k}, \vec{k}', L) = & \sum_{\zeta} \hat{S} \hat{J}^2 \hat{J}' \hat{k}_{\ell} \hat{L} (-1)^{J-J'-\ell+k_{\ell}} \begin{Bmatrix} \ell & \ell' & k_{\ell} \\ J & J' & L \\ S & S & k \end{Bmatrix} \\ & \times \langle k_{\ell} q_{\ell}, L\Lambda | kq \rangle \langle \ell' m_{\ell'}, \ell m_{\ell} | k_{\ell} q_{\ell} \rangle Y_{\ell' m_{\ell'}}(\vec{k}') Y_{\ell m_{\ell}}(\vec{k}) \\ & \times \sqrt{4\pi} Y_{L\Lambda}(\vec{P}) G^{LST}(\ell' J', \ell J, P) \end{aligned} \quad (17)$$

where the sum runs over $\zeta = \ell' J' \ell J m_{\ell'} m_{\ell} k_{\ell} q_{\ell} \Lambda$.

In our present application, these general formulæ can be simplified by making specific choices of the coordinate system for the description of the scattering angles. For a right handed coordinate system with \hat{z} along the projectile direction \hat{k} , \hat{y} along \hat{n} , and the momentum \vec{P} in the scattering plane at an angle θ_P , Eq. (17) reduces to

$$G_{kq}^{ST}(\vec{k}, \vec{k}', L) = \sum_{\zeta} \hat{S} \hat{J}^2 \hat{J}' \hat{k}_{\ell} \hat{L} (-1)^{J-J'-\ell+k_{\ell}} \begin{Bmatrix} \ell & \ell' & k_{\ell} \\ J & J' & L \\ S & S & k_S \end{Bmatrix} \quad (18)$$

$$\times \langle k_{\ell} q_{\ell}, L\Lambda | kq \rangle \langle \ell' q_{\ell}, \ell 0 | kq \rangle Y_{\ell' q_{\ell}}(\theta, 0) \hat{\ell} Y_{L\Lambda}(\theta_P, 0)$$

$$\times G^{LST}(\ell' J', \ell J, P)$$

The values of G^{LST} were calculated using

$$G^{LST}(\ell J \theta_P) = \frac{1}{\hat{j}^2} \left\{ \langle J0, L0 | J0 \rangle \langle \ell J M = 0 | G^{ST}(P) | \ell J M = 0 \rangle \right. \quad (19)$$

$$\left. + \sum_{M>0} (\langle JM, L0 | JM \rangle + \langle JM, L0 | J - M \rangle) \langle \ell J M | G^{ST}(P) | \ell J M \rangle \right\}$$

The angle-dependent transform was calculated as

$$G_{kq}^{LST} = \hat{L} \sum_{J\ell} \hat{J}^3 (-1)^{\ell} G^{LST}(\ell J \theta_P) \sum_{k_{\ell} q_{\ell} \Lambda} \hat{k}_{\ell} (-1)^{k_{\ell}} \begin{Bmatrix} \ell & \ell' & k_{\ell} \\ J & J & L \\ S & S & k_S \end{Bmatrix} \quad (20)$$

$$\times \langle k_{\ell} q_{\ell}, L\Lambda | kq \rangle \langle \ell' q_{\ell}, \ell 0 | k_{\ell} q_{\ell} \rangle Y_{\ell' q_{\ell}}(\theta, 0) Y_{L\Lambda}(\theta_P, 0)$$

and

$$G_C^{LST} = \hat{S}^{-2} G_{00}^{ST}(\vec{k}, \vec{k}', L) \quad (20)$$

$$G_{LS}^{L1T} = \frac{i\sqrt{3}}{6} G_{11}^{1T}(\vec{k}, \vec{k}', L) \quad (21)$$

$$G_{TD}^{L1T} = \frac{\sqrt{2}}{72} \left[3(1 - \cos \theta) G_{20}^{1T} + 2\sqrt{6} \sin \theta G_{21}^{1T} + \sqrt{6}(3 + \cos \theta) G_{22}^{1T} \right] \quad (22)$$

$$G_{TX}^{L1T} = \frac{\sqrt{2}}{72} \left[3(1 + \cos \theta) G_{20}^{1T} - 2\sqrt{6} \sin \theta G_{21}^{1T} + \sqrt{6}(3 - \cos \theta) G_{22}^{1T} \right]. \quad (23)$$

An additional transform was needed at the end to replace states where $S = 0, 1$ and $T = 0, 1$ with the singlet and triplet spin and isospin operators customarily used by the distorted-wave programs.

In Ref. [10], it was noted that the spherical Pauli operator gave results very close to the average over M values. The amplitudes obtained with $L = 0$ only also reproduce this same result.

Values of the density-dependent G -matrix calculated with the spherical Pauli operator were used for entries where $7 \leq J \leq 15$, matrix elements that we needed to specify the long-range pion tail of the NN interaction. No values of $J > 15$ were considered.

The amplitudes were then calculated at a number of values of θ and reproduced using a sum of Yukawa functions [5,23]. The matrix inversion scheme outlined in Ref. [5] again produces the solution in a single step.

Calculations were made for both $\theta_P = 0$ (along \hat{z}) and $\theta_P = \theta/2$. When the $L = 2$ terms were included in the NN scattering amplitudes for $\theta_P = \theta/2$, it was no longer possible to produce a high quality fit with the usual number of Yukawa coefficients. Instead, the direct and exchange parts of the interaction were allowed to have separate coefficients. In practice, the coefficient values for the direct and exchange expansions were close. Because the $L = 2$ contributions were much smaller than for $L = 0$, only $L = 2$ was considered and terms with $L \geq 4$ were ignored.

IV. Results for (p,p') reactions

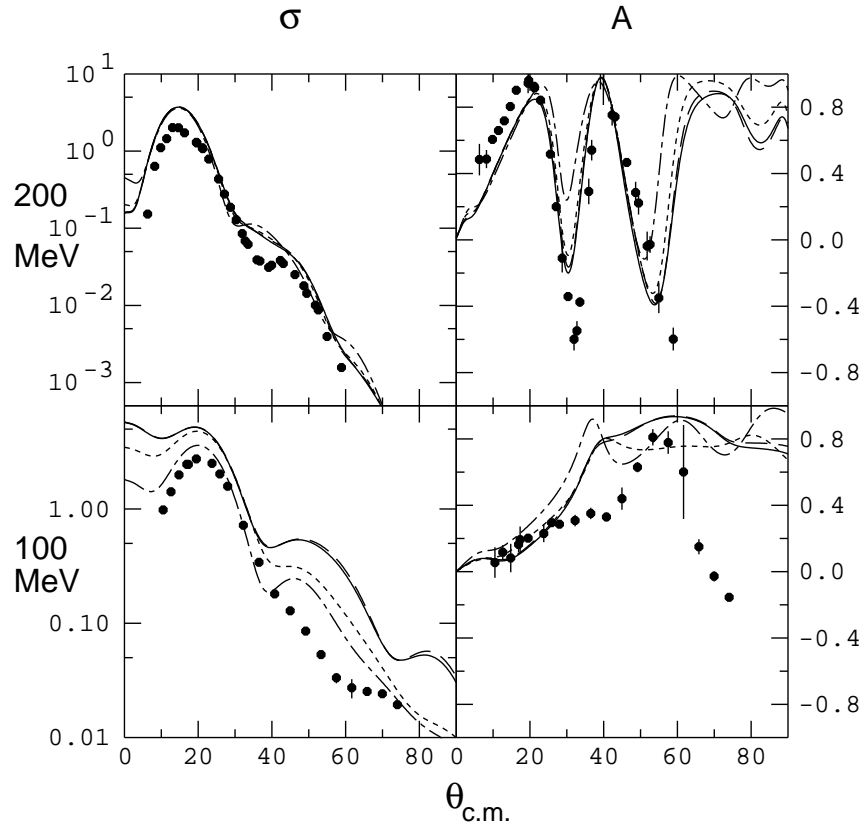


Figure 1: Measurements of cross section and analyzing power for the transition to the first 2^+ state at 6.917 MeV in ^{16}O at two bombarding energies, 200 and 100 MeV. The data are from Refs. [24,25]. The calculations use free (dash-dot), spherical Pauli (short dash), and exact Pauli interactions with \vec{P} along \hat{z} (long dash) or $\theta/2$ (solid).

In this section we will compare (p,p') calculations made with the two forms of the exact Pauli projection operator (quantized along \hat{z} or $\theta/2$) and representative sets of data. Figure 1 contains the cross section and analyzing power for the first 2^+ state in ^{16}O at

6.917 MeV. The 200-MeV data are from Ref. [24]; the 100-MeV data are reported in Ref. [25]. The calculations were made with the distorted-wave program LEA [26]. The transition formfactors reproduce the inelastic electron scattering measurements of Buti [27]. The distorted waves were calculated from a folded optical potential based on the same density-dependent interaction that is used for the transition. (Relativistic effects as described in Ref. [5] are not included.)

The changes made by including medium effects represented by the spherical Pauli blocking operator as compared with no medium effect is represented by the difference between the short-dashed (spherical Pauli) and dash-dot (free) curves. At 200 MeV, changes are noticeable only at the largest angles in the analyzing power. Including Pauli blocking increases the size of the diffractive oscillations, a change that goes in the direction toward better agreement. If the angle averaged operator is replaced by the exact operator, only small additional changes result [medium dash (solid) has \vec{P} along \hat{z} ($\theta/2$)]. There is almost no effect from the choice of system momentum.

At 100 MeV, the Pauli blocking medium effects are larger. In this case the change from the spherically averaged to the exact operator makes a much larger difference, especially for the cross section. This is in keeping with the expectation that as the projectile momentum goes down, a greater fraction of the scattered states will be eliminated from consideration by the step functions of Eq. (5), and the procedure for doing this will matter more. Compared to the change wrought by using the exact operator, the choice of system momentum still appears not to matter. This test demonstrates that, especially near 100 MeV, the exact treatment of the Pauli blocking operator is important for an accurate description of medium effects.

The choice of the momentum of the system depends on the most appropriate model for the exchange in a (p,p') transition. Transitions where exchange is important are the reactions to the 0^- states. For the $0^+ \rightarrow 0^-$ spin combination, only the spin-longitudinal term in the interaction can contribute. In a plane-wave calculation, the analyzing power is non-vanishing only if the exchange is included in finite range. In order to handle this properly, the calculations were made with the distorted-wave program DWBA86 [28]. Figure 2 shows the same set of curves as Fig. 1 for the 200-MeV cross section for the $T = 0, 0^-$ state at 10.957 MeV in ^{16}O . The data are from Ref. [29]. The solid (\vec{P} along $\theta/2$) curve is now substantially different from the medium dash (\vec{P} along \hat{z}) curve. (The normalization of the cross section is arbitrary as electron scattering is not sensitive to this transition and there is no other reference that precisely constrains the structure.) This demonstrates that there is a sensitivity to the choice of system momentum for transitions that depend on the treatment of exchange.

Similar tests were conducted for measurements of the polarization transfer coefficients for unnatural parity transitions at 200 MeV [14]. In this case the formfactor for these transitions is peaked at a large radius and Pauli blocking effects of any form are suppressed.

V. Conclusions

As the basis for (p,p') reaction calculations, we have used a G -matrix that is generated from an exact treatment of the angular dependence of the Pauli exclusion operator. For

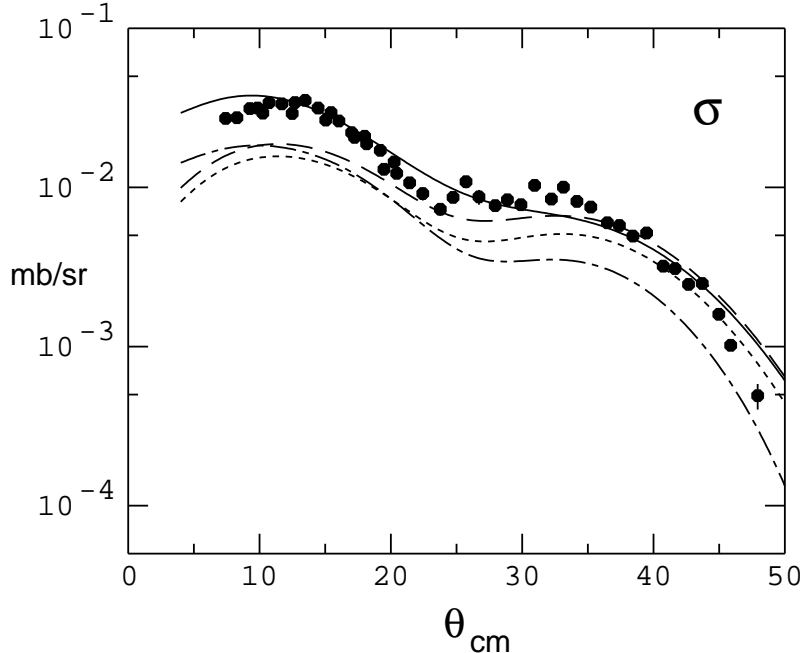


Figure 2: Measurements of the cross section for the transition to the $T = 0, 0^+$ state at 10.957 MeV in ^{16}O . The 200-MeV data is from Ref. [29]. The curves are described in Fig. 1.

proton energies near 100 MeV, lifting the spherical averaging approximation makes significant changes to the (p,p') cross section and analyzing power. The exact treatment should be used whenever precise Pauli exclusion medium effects are considered. This becomes less important as the projectile energy rises.

One consideration of exchange in the coordinate space distorted-wave calculation leads to the choice of the system momentum that is not along the incident projectile direction. Transitions that are sensitive to tensor forces or finite-range exchange may be sensitive also to the angle of this system momentum, even at the higher energies.

The authors acknowledge financial support from the U.S. National Science Foundation under grant number PHY-0100348 (E.J.S.) and the U.S. Department of Energy under grant number DE-FG03-00ER41148 (F.S.).

- [1] H.V. von Geramb, *The Interaction Between Medium Energy Nucleons in Nuclei – 1982*, AIP Conf. Proc. No. 97 (AIP, New York, 1983) p. 44.
- [2] L. Rikus, K. Nakano, and H.V. von Geramb, Nucl. Phys. **A414**, 413 (1984).
- [3] K. Nakayama and W.G. Love, Phys. Rev. C **38**, 51 (1988).
- [4] K. Amos, P.J. Dortmans, H.V. von Geramb, S. Karataglidis, and J. Raynal, Adv. Nucl. Phys. **25** 275 (2000).
- [5] F. Sammarruca, E.J. Stephenson, and K. Jiang, Phys. Rev. C **60**, 064610 (1999).
- [6] M.I. Haftel and F. Tabakin, Nucl. Phys. **A158**, 1 (1970).
- [7] T. Cheon and E.F. Redish, Phys. Rev. C **59**, 331 (1989).

- [8] E. Schiller, H. Müther, and P. Czerski, Phys. Rev. C **59**, 2934 (1999); **60**, 059901 (1999).
- [9] K. Suzuki, R. Okamoto, M. Kohno, and S. Nagata, Nucl. Phys. **A665** 92 (2000).
- [10] F. Sammarruca, X. Meng, and E.J. Stephenson, Phys. Rev. C **62**, 014614 (2000).
- [11] A.A. Ioannides and R.C. Johnson, Phys. Rev. C **17**, 1331 (1978).
- [12] E.J. Stephenson, C.C. Foster, P. Schwandt, and D.A. Goldberg, Nucl. Phys. **A359**, 316 (1981).
- [13] E.J. Stephenson, J.C. Collins, C.C. Foster, D.L. Friesel, W.W. Jacobs, W.P. Jones, M.D. Kaitchuck, P. Schwandt, and W.W. Daehnick, Phys. Rev. C **28**, 134 (1983).
- [14] F. Sammarruca, E.J. Stephenson, K. Jiang, J. Liu, C. Olmer, A.K. Opper, and S.W. Wissink, Phys. Rev. C **61**, 014309 (1999).
- [15] J.J. Kelly and S.J. Wallace, Phys. Rev. C **49**, 1315 (1994).
- [16] F. Sammarruca and E.J. Stephenson, Phys. Rev. C **64**, 034006 (2001).
- [17] R. Machleidt, Adv. Nucl. Phys. **19**, 189 (1989).
- [18] K.A. Brueckner, C.A. Levinson, and H.M. Mahmoud, Phys. Rev. **95**, 217 (1954).
- [19] H.A. Bethe, Phys. Rev. **103**, 1353 (1956).
- [20] J. Goldstone, Proc. R. Soc. London, Ser. A **239**, 267 (1957).
- [21] H.A. Bethe, Annu. Rev. Nucl. Sci. **21**, 93 (1971).
- [22] V.G.J. Stoks *et al.*, Phys. Rev. C **49**, 2950 (1994).
- [23] W.G. Love and M.A. Franey, Phys. Rev. C **24**, 1073 (1981).
- [24] H. Seifert *et al.*, Phys. Rev. C **47**, 1615 (1993).
- [25] H. Seifert, Ph.D. thesis, University of Maryland, 1990.
- [26] James J. Kelly, Program Manual for LEA, 1995.
- [27] T.N. Buti *et al.*, Phys. Rev. C **33**, 755 (1986); and references therein.
- [28] R. Schaeffer and J. Raynal, program DWBA70; S. Austin, W.G. Love, J.R. Comfort, and C. Olmer, extended version DWBA86 (unpublished).
- [29] R. Sawafta, private communication.